

# Detecting Network-based Internet Censorship via Latent Feature Representation Learning

Shawn P. Duncan<sup>a</sup>, Hui Chen<sup>a,b</sup>,

<sup>a</sup>Department of Computer & Information Science, CUNY Brooklyn College, 2900 Bedford Avenue, Brooklyn, 11210, NY, USA

<sup>b</sup>Department of Computer Science, CUNY Graduate Center, 365 5th Avenue, New York, 10016, NY, USA

## Abstract

Internet censorship is a phenomenon of societal importance and attracts investigation from multiple disciplines. Several research groups, such as Censored Planet, have deployed large scale Internet measurement platforms to collect network reachability data. However, existing studies generally rely on manually designed rules (i.e., using censorship fingerprints) to detect network-based Internet censorship from the data. While this rule-based approach yields a high true positive detection rate, it suffers from several challenges: it requires human expertise, is laborious, and cannot detect any censorship not captured by the rules. Seeking to overcome these challenges, we design and evaluate a classification model based on latent feature representation learning and an image-based classification model to detect network-based Internet censorship. To infer latent feature representations from network reachability data, we propose a sequence-to-sequence autoencoder to capture the structure and the order of data elements in the data. To estimate the probability of censorship events from the inferred latent features, we rely on a densely connected multi-layer neural network model. Our image-based classification model encodes a network reachability data record as a gray-scale image and classifies the image as censored or not using a dense convolutional neural network. We compare and evaluate both approaches using data sets from Censored Planet via a hold-out evaluation. Both classification models are capable of detecting network-based Internet censorship as we were able to identify instances of censorship not detected by the known fingerprints. Latent feature representations likely encode more nuances in the data since the latent feature learning approach discovers a greater quantity, and a more diverse set, of new censorship instances.

**Keywords:** Internet censorship, Internet censorship detection, Network-based Internet censorship detection, Deep neural network, Feature representation learning

## 1. Introduction

This study focuses on a particular type of Internet censorship called *network-based Internet censorship*, i.e., the impairing or blocking of access to online content and service *intentionally* by the network, a *third party* between the user host and the online content and service provider [1], where an example of the online content can be a blog post on the Web [2] and that of the service can be the Virtual Private Network (VPN) service [3]. Figure 1 illustrates this concept. This type of censorship needs the control of neither the user hosts and applications nor the content and service providers. Rather it requires the access to the network components, such as, routers and DNS servers between the user hosts and the content and service providers. It is prevalent among those, such as a state actor, who seek to block or impair access to politically, culturally, or religiously sensitive content hosted on a server within or out of its jurisdiction without a need to tamper with the user hosts, the user applications, and the content servers.

The network-based Internet censorship can lead to network outages [4]. Differentiating the censorship events from other types of outages can thus benefit the design and implementation of Internet network architecture, protocols, and systems [1, 5]. Understanding the censorship mechanism can also help develop circumvention techniques [6–8].

Aside from these technical perspectives, there have been pursuits to gauge its social, political, cultural, and religious implications [9–11]. These works reveal the complexity and the intricacy of Internet censorship, which sometimes challenges conventional wisdom given its prevalence among countries, politics, cultures, and religions of a great spectrum [10, 12–19].

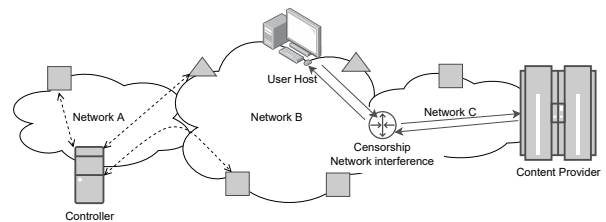


Figure 1: Network-based Internet censorship and measurement. Network-based Internet censorship takes place at neither the user host (or the application on the host) nor the content provider. To gauge such censorship, a measurement platform sets up vantage points, depicted as squares and triangles in the figure. The controller of the platform instructs the vantage point to send a network request to the content server or sends a request appearing from the vantage point to the content server. Although the existing platforms adopt more complex methods, a straightforward method to detect censorship, e.g., whether Network B censors a network request is to compare the network traces from multiple vantage points. Following that, we can design a fingerprint for the network trace for the censored vantage point and the content provider.

In order to study censorship prevalence and mechanisms sys-

tematically, to understand this global phenomenon, to improve the Internet infrastructure given the prevalence of it, prior efforts have led to the design, implementation, and deployment of large scale Internet measurement platforms. Internet censorship manifests as a network reachability problem, i.e., the users are unable to access the content or the service, or are accessing the content or the service at a severely degraded quality of service. These platforms are designed to collect network measurement data about network reachability, and further, to detect Internet censorship events from the reachability data [20–22]. As shown in Figure 1, these measurement platforms typically set up vantage points, strategically or sometimes opportunistically selected monitoring hosts on the Internet. The platforms typically have controller hosts (that the platforms may name differently) and the controllers have network requests sent to the content providers from or appearing to originate from the vantage points.

These measurement platforms produce a large amount of network reachability data [20, 21]. There are challenges to detecting censorship events from the reachability data, such as, the platforms must process the amount of data, and they also need to find a way to infer whether the reachability problem is intentional to differentiate a censorship event from an ordinary network outage. These works generally rely on a rule-based approach to detect censorship, such as, by matching the measurement data to censorship fingerprints that are usually purposefully designed regular expressions [20, 21]. The rule-based approach has several advantages, such as, it is computationally efficient to execute a rule, and a carefully designed rule is also unlikely to have a false detection. However, the rule-based approach has several disadvantages. First, it requires significant technical expertise. Second, it is laborious to add new rules. Third, it cannot detect any Internet censorship not described by existing rules.

Machine learning-based approaches have found applications in software and system quality assurance and security [23, 24]. An improvement over the rule-based approaches where the rules are pre-defined by human experts manually, the learning-based approaches automatically learn “rules” or “patterns” in the relevant data. As a result, they can not only offer better predictive performance than the rule-based systems, but also reduce human efforts required to design rules for the rule-based systems. Learning-based approaches are making inroads in both the design of censorship mechanisms and the data analysis and detection of censorship [25, 26]. Thus far, for network-based Internet censorship detection, most prior work uses machine learning algorithms in a semi-automated fashion. For instance, clustering algorithms are used to group *block pages*, notices that content providers respond to the users to explain the unavailability of requested content [27]. A necessary condition to the learning-based approaches (including clustering) is to express the network reachability data in a form, i.e., a representation of data, suitable for machine learning algorithms. This requires us to decide how we extract and represent features from the data. One approach is to borrow features from natural language processing, such as, to use features like page length and term-frequency [21, 27]. Another is to borrow approaches from

image recognition, such as, to extract feature representations as screenshots of block pages using ResNet50, a pre-trained convolutional deep neural network [44].

Limitations of the prior learning-based approaches for network-based Internet censorship are two. First, the simple features like page length and term-frequency do not sufficiently capture nuances in the network reachability data, e.g., block pages, which results in a high false positive rates [15]. Second, the prior work primarily uses the learning algorithms to aid the censorship detection rule design. One example is FilterMap [44]. It extracts feature representations from screenshots of block pages using ResNet50 and clusters block pages into approximately 200 groups of block pages. Following this, the researchers manually design detection rules (signatures of block pages) by examining each group of block pages. Another example is ICLab [21]. It computes the term-frequencies of HTML tags and the Locality Sensitive Hashing index of the text in block pages, produces 48 block page clusters that are similar either in HTML structures or in page text. Again, the researchers manually design new signatures for these clusters in the form of regular expressions.

Despite these limitations, the prior work has led to the creation of hundreds of network-based censorship fingerprints in the form of regular expressions and discovered new censorship events [20, 21]. In addition, the work also results in the accumulation of a large amount of reachability data labeled with censorship types according to the signatures. Taking advantage of these and motivated by the recent development in deep learning, we present and evaluate a censorship detection approach that is built upon well-known deep learning techniques. The contributions of this work are as follows:

1. The work results in an “end-to-end” censorship detection system that automates the entire process of censorship detection. On one end, the system automatically learns latent features from network reachability data records, which yields feature representations of the records. On the other end, from the feature presentations, we determine whether a network reachability problem is a censorship event via a classification model. The system therefore eliminates the need manually to design machine learning features and reduces the manual effort to detect new censorship events.
2. The network reachability data contains structures and pieces of some data elements appear in a particular order. Observing the characteristics of the data, we design the feature presentation learning model to be a sequence-to-sequence model adapted from natural language processing.
3. The proposed classification model is a supervised learning model. Supervised learning models require a large set of labeled data to train, e.g., a known set of network measurement records that are labeled as censored or uncensored. Our results show that the proposed supervised learning models trained using the block pages labeled by known censorship fingerprints can recognize both known and new censorship events. As a result, we hypothesize that there is additional information in the labeled block

pages beyond what the signatures capture.

4. To evaluate the above end-to-end censorship detection approach and to explore the design space, we design an alternative detection approach that treats network reachability data records as gray-scale images and train a state-of-the-art deep learning image classification model to recognize the images as censored or not. To compare the two proposed approaches, we process a large collection of Censored Planet block page records. The end-to-end approach appears to have an advantage over the alternative due in part to the sequence-to-sequence feature representation learning.
5. This work also results in a library of Python scripts that can be used for replication and future research. The authors make this library publicly available.

We structure the rest of this article as follows. To situate the proposed work, we discuss related work in Section 2. We introduce our proposal, the latent feature representation based approach and the image-based alternative in Section 3. In Section 4, we evaluate the proposed approaches. Our work isn't without limitations. We dedicate Section 5 to a discussion of the limitations and the threats to validity. Finally, we conclude this work in Section 6.

## 2. Related Work

*Internet Censorship.* Internet Censorship has been a global phenomenon, which has attracted a sustained research interest and resulted in a plethora of literature. A significant body of the literature is to understand the prevalence of censorship, such as, to measure the online content, the network protocols and applications, and the geographical regions that are subject to censorship [10, 12–19]. Another is to unpack the censorship mechanisms, such as, IP-based blocking, TCP packet injection, Transparent proxy, DNS manipulation, and SNI filtering [1, 7, 17, 21].

This work is not aimed to expand these bodies of knowledge. Instead, our focus is about the design of the “end-to-end” network-based Internet censorship detection system by leveraging the recent advances in deep learning and a wealth of network reachability data collected by the large scale Internet measurement platforms.

*Censorship Measurement Platforms.* Large scale remote network measurement platforms for studying Internet censorship have emerged over the last decade. [20–22, 29–33, 44]. These platforms fall into two broad categories with regard to the measurement methods employed and the selection and use of vantage points.

Some platforms like OONI [22], ICLab [21], and Disguiser [33] use a mixture of volunteer hosts, selected VPN servers, SOCKS Proxies, or RIPE Atlas servers as vantage points. From these vantage points the platforms make attempts to access a brand range of content and services on the Internet, typically *like an ordinary user would do*, and collect reachability data.

Platforms like Censored Planet [20] take a different approach. Using systems like Augur [29], Iris [30], Satellite [31], Quack [32], and HyperQuack [44], these platforms rely on *network side-channels* to gauge potential network censorship events. The distinction here is that ordinary users would not access online content and services via these side-channels; however, the platforms can select servers that support the side-channel measurement mechanism globally as the vantage points. These two categories of platforms are complementary. For instance, Censored Planet can select far more vantage points to provide a more complete geographical and network coverage and continuity than OONI and ICLab [20]; however, the censorship mechanisms that are applied to ordinary network traffic may not be always applicable to the network side-channels, and as such, Censored Planet may not be able to detect some Internet censorship events, which can lead to higher false negative rate than OONI and ICLab [21].

The platforms are the foundation and the motivation of this work. First, these platforms are continuously collecting network measurement data, which provides a foundation for the proposed data-driven Internet censorship detection systems using deep neural networks. Second, the platforms have made available a large collection of censorship fingerprints, e.g., Censored Planet makes available a tool to scan the collected data records to match a set of known censorship fingerprints. Our system adopts a supervised learning model to classify network reachability data records, and for this the fingerprints and the tool are particularly useful to create labeled training data set for the classification model. Third, some platforms use machine learning, particularly, unsupervised learning to cluster network reachability data records to design new censorship fingerprints [21, 44], which is a laborious process and requires human expertise. This observation motivates us to propose the end-to-end network-based Internet censorship detection systems.

For this work, we elect to use the Censored Planet data set to study the proposed approaches to detect network-based Internet censorship. Censored Planet is distinct in that the platform collects network measurement data on network side-channels. The censorship measured is therefore network-based censorship other than host and server-based censorship [1] — an exception may be censorship mechanism deployed on host-based network filters or firewalls.

*Machine Learning for Censorship Detection.* Our work is a machine learning-based approach for censorship detection. There are studies that propose machine learning approaches for censorship detection. For instance, a study uses machine learning to understand Chinese social media censorship [26]. However, these approaches are for the host-based or the server-based censorship because the data used in their studies are the content of the blogs being censored. Different from those, our work is on network-based Internet censorship detection in that the data on which our approaches rely are network measurement data and do not include the online content being censored.

Additionally, machine learning has been used to design sophisticated Internet censorship methods or to recognize cer-

tain types of network traffic [25, 34]. This trend adds urgency to studies on machine-learning based censorship detection like this one. This necessity of this work is increased given that the literature on detecting network-based Internet censorship using machine learning is still rare.

*Learning from Network Measurement Data.* This work is about learning from the network reachability data collected by censorship measurement platforms to detect Internet censorship. The network reachability data is a type of network measurement data. A deep learning model has been used to characterize Internet hosts. In particular, a variational autoencoder, an unsupervised neural network model, was previously designed to construct low-dimensional embeddings of the high-dimensional binary representations of the IP intelligence data collected by Censys, a type of network measurement data [35]. Our work significantly benefits from this and in spirit is an application of such an approach. However, there are several differences. First, the problem we investigate, network-based Internet censorship detection, is distinct from host characterization. Second, our approach to infer the low-dimensional embeddings is a sequence-to-sequence model, which is motivated by the observation that the order of data elements matters. Third, we compare the latent feature representation approach with a state-of-the-art image-based approach. Finally, we design an engineering solution to overcome the hurdle that the censorship network measurement data are enormous.

### 3. Censorship Feature Representation and Detection

We propose an end-to-end network-based Internet censorship detection system whose processing pipeline is as shown in Figure 2a. The pipeline begins with converting network reachability data to numerical vectors, i.e, raw vectors as detailed in Section 3.1. We design a sequence-to-sequence autoencoder model as the next processing component in the pipeline, and it is to infer latent feature representation in embedding space (called embedding vectors) from the raw vectors. We discuss this component in Section 3.2. Finally, we classify each embedding vector by a fully-connected neural network, which we present in Section 3.3. For convenience, we refer to this system as the E2ECD model. To evaluate this proposed system, we propose an alternate one as in Figure 2b and document it in Section 3.4.

#### 3.1. Structured and Textual Data to Numerical Vectors

The censorship measurement platforms run tests to collect network reachability data. A test typically consists of a request and a response where a no-response or timeout event is considered a response. There are *three challenges* to process the data collected by the measurement platforms. First, the network reachability data recorded by the censorship measurement platforms are large and overwhelm our local storage capacity, and likely that of other researchers who wish to pursue a similar research agenda. Second, the requests and responses are structured data. For instance, Censored Planet runs HyperQuack

tests where a test consists of an Echo request and a response, and records the request and the response in the JSON format. Figure 1 is an example data record. As shown, the entire data record is structured. Furthermore, the values of some data fields are either structured or semi-structured. For instance, the numbers in an IP address have different meaning as the address has both host number and network number while the response field can be in several formats, such as, in HTML with embedded JavaScript (as illustrated in Listing 1). Third, the combination of the overwhelming amount of data and the feature representation learning via deep neural networks can demand excessive computational resources, and thus there is need to balance feature representation learning effectiveness and required computational resources.

```

1 {
2   "vp": "114.116.151.108",
3   "location": {
4     "country_name": "China",
5     "country_code": "CN"
6   },
7   "service": "echo",
8   "test_url": "666games.net",
9   "response": [
10    {
11      "matches_template": false,
12      "response": "HTTP/1.1 403 Forbidden\n
13      nContent-Type: text/html; charset=utf-8\n
14      nServer: ADM/2.1.1\n
15      nConnection: close\n
16      nContent-Length: 520\n
17      \n<html>\n<head>\n<meta http-equiv=\n
18      \"Content-Type\" content=\n
19      \"text/html; charset=GB2312\" /\n
20      \n<style>body{background-color:#FFFFFF}\n
21      \n<title>\u975e\u6cd5\u963b\u65ad222\n
22      \n</title>\n<script language=\n
23      \"javascript\" type=\n\"text/javascript\"\n
24      >\nwindow.onload = function () {\n
25      \ndocument.getElementById(\n
26      \"mainFrame\").src = \"http://114.115.192.246:9080/error.html\";\n
27      }\n</script>\n</head>\n<body>\n
28      \n<iframe style=\n\"width:100%; height:100%;\n
29      \" id=\n\"mainFrame\" src=\n\"\" frameborder=\n
30      \"0\" scrolling=\n\"no\"/>\n</body>\n</html>\n",
31      "start_time": "2021-07-19T01:07:35.692415469-04:00",
32      "end_time": "2021-07-19T01:07:37.135588863-04:00"
33    },
34    ],
35   "anomaly": false,
36   "controls_failed": false,
37   "stateful_block": false,
38   "tag": "2021-07-19T01:01:01"
39 }

```

Listing 1: An example of HyperQuack test data record. We truncated the record to save space. The response field is an array, and as such, an actual record can have multiple response bodies, where each response body corresponds to a block page; however, we transform each of those records to multiple records, each of which has a single response body. See Section 4.1 for detailed discussion.

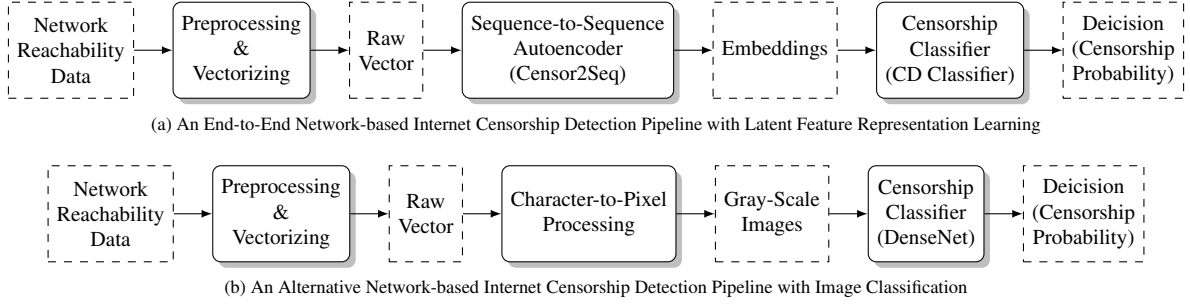


Figure 2: Processing pipelines of proposed models

*Streaming I/O for Large Scale Machine Learning.* To address the overwhelming amount of data records, we opt for an engineering solution that can iterate through the data directly from their cloud storage and process the data records as a data stream. Our engineering solution based on WebDataset [36] is publicly available as a Python module [37].

*Vectorizing Structured Data.* Our aim here is to capture nuances from the structured network measurement data records, and at the same time produce relatively small input vectors, which is driven in part to address the latter two challenges discussed above.

An example of the Censored Planet measurement data record is given in Listing 1. Each record can have multiple responses for a test request value. Because of this, to begin to process such test data, we pair the top level metadata corresponding to a request to each unique response to form a test record. Such data records are structured as it follows a tree-like structure as dictated by its syntax, e.g., in JSON syntax and contains multiple data types of data. As required by machine learning models, we need to transform each test record to a numerical vector [35]. It is important to note that we treat a test record as a sequence in order to preserve the structure of the field values. We generally follow the spirit of the prior method that parses JSON data records [35] to transform test records to sequences in a consistent and predictable manner, however with several distinctions that we detail below. The end result is a set of numerical vectors. For convenience, we refer to the numerical vector of a test record as the vector representation of the record or the raw vector.

The transformation method is as follows. First, we process simple data fields, e.g., Datetime fields in ISO format are transformed to UNIX timestamps, Boolean fields transformed to a 1 or 0, and we split and convert the IP addresses into sequential integers. We hold all this simple integer data and encode it as described below. Second, two fields that contain text, `test_url` and `response` need a more specialized approach. The `response` field can contain the HTTP response code and string, the HTTP headers, and the markup of a block page with text in a variety of languages, e.g., the `response` field in the example in Figure 1 is a concatenation of the response code and string concatenated, the HTML headers, and HTML that contains an embedded JavaScript. Some versions of Censored Planet data separate these elements into their own fields within

a nested JSON object. We concatenate the `test_url` followed by the `response` data into a single string. This string is relatively long when compared to the rest of the field. Aiming to reduce smaller input vectors, we then take advantage of the XLM-R multilingual transformer model to process this string into numeric tokens [38]. Figure 3 illustrates the processing pipeline for these data fields.

The XLM-R transformer uses just over 250,000 tokens. Given the amount of the data records we process, the demand of both memory and CPU time during feature representation learning is unbearable. We reduce the size of the token vocabulary so that the training tasks would fit within the computing capacity available to us. We do this by creating a sequential index of the 6,813 XLM-R tokens needed to encode all the text in our datasets. We use the index value in our vectors rather than the corresponding XLM-R value. The maximum value in our simple integer data described above is 256. We encode these integers as tokens also, so there are 7,069 possible token values which is substantially smaller than XLM-R vocabulary. The final raw vector begins with the variable length encoded text which begins with XLM-R sequence start and sequence end tokens. Appended to this variable length data are the simple integer tokens which are also surrounded by XLM-R sequence start and sequence end tokens.

### 3.2. Feature Representation Learning

The next step in our method is to learn latent feature representations from the raw vectors. For this we build an unsupervised sequence-to-sequence neural network model. For convenience, we call this model Censor2Seq.

The latent feature representations are often referred to as embeddings [35]. The learning here is essentially to determine an embedding function  $E : X \rightarrow Y$  that takes an input  $x \in X$  in a  $m$ -dimensional space and produces its corresponding numerical vector  $y \in Y$  in a  $n$ -dimensional vector space, where  $n \ll m$ . The advantage of the embeddings are well discussed in the literature [35]. A primary advantage is that a well-designed low-dimensional embedding function can infer embedding vectors that retain information in raw input data in much higher dimension and offers significant computational advantage due to low dimensionality and the continuity of the embedding space.

We follow the typical encoder-decoder architecture [35, 39] to design the feature representation learning model. The architecture of the model is in Figure 4. The model takes the raw

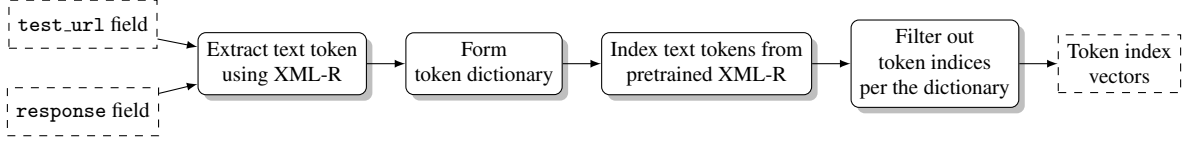


Figure 3: Multilingual data processing of the `test_url` and `response` fields and dimensionality reduction via a pretrained XLM-R model [38]. The `response` field can contain natural language text and program code. To reduce the size of the encoding vectors, We filter out those with low frequency, such as, those do not appear in our data (i.e., frequency is 0) or rarely appear depending on the constraint of the available computational resources. In this work, by filtering out tokens with frequency of 0, we reach sufficiently small embedding vectors of length of 6,813.

numerical vectors as input. Each vector is a sequence of tokens, the set of tokens of all the row vectors is the “vocabulary”, and each token is represented by an integer that indexes the token in the vocabulary. The model consists of an encoder block, a decoder block, and a predictor block.

The predictor is straightforward. The inputs to the predictor are the concatenated vector of a weighted context vector ( $\vec{c}$ ) and the state vector ( $\vec{h}$ ) of the decoder block that we shall discuss later. The predictor outputs a series of probabilities ( $\vec{p}$ ) across the range of possible tokens, representing a discrete probability mass function over the vocabulary. The weighted context vector here is to capture the importance of different source-side information (e.g., which element in the state vector) for predicting the probability of a particular token in the vocabulary [40]. We shall give a more detailed treatment of the context vector below (See the discussion about Equation (2)). These probabilities are then used to compute a cross-entropy loss at each step in the decoding process. The summation of these losses for all decoding steps is used as the loss for the current input. The cross-entropy loss function is well-known and is estimated as follows,

$$\mathcal{L}(\mathbf{x}, \mathbf{p}) = -\frac{1}{m} \sum_{i=0}^{m-1} \sum_{t=0}^{T-1} p_i(x_{it}) \quad (1)$$

where  $\mathbf{x}$  represents the batch of training data consisting of  $m$  raw vectors of censorship test records,  $\vec{x}_i$  the  $i$ -th vector of  $\mathbf{x}$ ,  $x_{it}$  the  $t$ -th item of  $\vec{x}_i$ ,  $p_i(\vec{x}_{it})$  its probability mass, and  $T$  the length of  $\vec{x}$  or the total time steps.

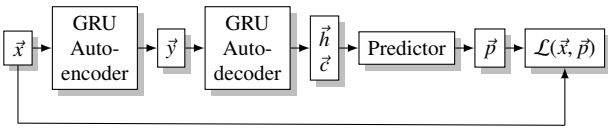


Figure 4: The architecture of the encoder-decoder model for sequence-to-sequence feature representation learning where  $\vec{x}$  is a raw vector in a high-dimensional space,  $\vec{p}$  is akin to an estimate of  $\vec{x}$ ,  $\vec{y}$  is the embedding vector in a low-dimensional embedding space, and  $\mathcal{L}$  is the loss function. The learning algorithm is to minimize  $\mathcal{L}$ .

The encoder is a bidirectional Gated Recurrent Unit (GRU). It takes a vector representation as input and outputs a sequence of states, i.e.,  $h_t$  at time step  $t$ . The final state summarizes the entire vector representation and is the embedding of the test record, i.e.,  $\vec{y}$  in Figure 4. Note that  $\vec{y} = h_{T-1}$  where  $T-1$  is the last time step.

The complexity of the model is in the decoder where we take advantage of several mechanisms to help with training speed

and convergence. The decoder takes the output of the encoder (i.e.,  $\vec{y}$ ) as input and attempts to restore the input to its original form (i.e.,  $\vec{x}$ ).

First, before processing an input sequence, we use a simplification of scheduled sampling [41, 42]. This sampling selects the inputs for the decoder by randomly switching between *auto-regression* and *teacher forcing*. The difference between these two strategies begins with the second item of the input sequence (i.e.,  $\vec{y}$ ). If auto-regression has been chosen the inputs will be sampled from the range of the vocabulary using the probabilities produced by the predictor block (i.e.,  $\vec{p}$ ). If teacher forcing is chosen, the decoder inputs are the same as the inputs to the encoder.

The decoder is a sequence of bidirectional Gated Recurrent Unit Cells. We enhance it with an attention mechanism [43], in particular, the “dot” attention mechanism [40]. Instead of using fixed neuron weights, the attention mechanism allows us to enhance the effect of some parts of the input data while diminishing other parts for predicting token probabilities via attention scores. In one direction, each token in the input sequence is processed through the GRU cells. In the other direction, we calculate attention scores. Attention scores are computed using a dot product [41]

$$score(h_t, c_t) = \frac{h_t^T \cdot c_t}{\sqrt{H}} \quad (2)$$

with values of  $h_t$  taken from the state produced at step  $t$  by the encoder,  $h_t^T$  is  $h_t$ ’s transpose,  $c_t$  is the context, and  $H$  is the input size used for the GRU Cell. We compute  $c_t$  as the decoder output at step  $t$ . We use the attention scores to weight the input sequence at each step of the decoding process.

The use of the model consists of two phases, training and inference. Given a set of vector representation of the test records, we train the model by minimizing the entropy loss function in equation (1). With a trained model, we infer the embedding of a test record by feeding the model with the numerical vector representation of the test record and take the output of the encoder as the embedding. The model is an unsupervised learning model during training and inference, and as such, no labels of censorship are given.

### 3.3. Censorship Classification

An advantage of embedding is its versatility, due in part to the continuity of the embedding space. It can be fed to a variety of machine learning models. The central question we want to answer is, “is the reachability problem the result of censorship?”

For this purpose, we construct a multiple-layer fully-connected dense neural network with three layers as a binary classifier: an input layer matching the dimension of the embeddings produced by the autoencoder, an output layer that further refines the output of the hidden layer to a probability, and a hidden layer in between. For convenience, we call this neural network the CD classifier.

### 3.4. Alternative Approach

Prior works typically adopt a semi-automated approach for Internet censorship detection, where they first leverage an unsupervised machine learning algorithm, such as, a clustering algorithm to divide Internet outage measurements, e.g., block pages into clusters, and second, manually examine the clusters to determine whether the cluster represents a type of Internet censorship [21, 44]. A necessary step in the process is to extract data features from the internet measurement data. Page length and term frequency vectors are two features borrowed from natural language processing to cluster block pages [27]. Although the clustering algorithm using the two features reduces manual efforts to examine the clusters, several follow-up studies indicate that the features can lead to high false positives due to natural variations in page length from dynamic and language-specific content [15, 44]. Recognizing the limitation of the two features, researchers are seeking different feature representation methods for Internet measurement data, such as, block pages [44].

Deep learning has found tremendous success in computer vision [45, 46]. In contrast to more traditional learning algorithms, such as, Super-Vector Machine and Tree-based algorithms (Decision Tree, Random Forest) for which we need to extract from the raw data manually designed features to represent the data in a tabular form, deep learning can learn to extract features directly from the raw data, which, numerous studies show it is an advantage because we do not always know what the best features might be for a particular machine learning application [?]. A clever way to design a learning system for non-tabular data is to take advantage of these recent advances in deep learning by encoding the data as gray-scale images and use a deep learning model for computer vision that is readily available to learn from these images. There have been applications of this approach in several domains, such as, for malware detection [47] and for software defect prediction [48]. A gray-scale image can be encoded using a byte pallet, in which the range from black to white is encoded as an integer between 0 and 255. In other words, we can consider a gray-scale image as a vector of  $W \times H$  integers where  $W$  is the width of the image and  $H$  the height. For our structured data, after converting a censorship test record similar to that in Listing 1 into a raw vector, we pad the beginning and end of the vector with sufficient 0 to equal a uniform length of size  $W \times H$ . We then export this vector to a sequence of bytes, reshape the vector to a  $W \times H$  array from which we form the gray-scale image.

Recently several works have adopted this approach in their semi-automated censorship detection pipeline and find that the approach leads to improved predictive performance than those using the page length and term frequency vector features [20, 44]. Following these prior works, we build a fully-automated

Internet censorship detection model where we use images as feature representations of block pages. For this, we elect to use the well-known DenseNet model [45]. DenseNet uses the architecture of a Convolutional Neural Network (CNN). A DenseNet has multiple CNN blocks that have the following neuron connectivity pattern: each layer in the CNN block is connected to all the others with the block. Due to this connectivity pattern, there is a shortcut path between each individual layer to the loss function and the training of the layer can be directly supervised by the loss function. Aside from this, the connectivity pattern also results in a compact network that is less prone to overfitting and encourages heavy feature reuse. Because of this, prior work suggests that DenseNet should be a natural fit for per-pixel prediction problems [49].

DenseNet is available as a pre-trained model [50] that expects images sized  $224 \times 224$ . The pre-trained model has a final linear layer of size 1,000 as a classifier for 1,000 image categories. We replace that linear layer in the pre-trained model with a new layer accepting the same input dimension but producing a single output, the probability at which the input is a censorship event.

As an alternative to for the proposed End-to-End Censorship Detection model (E2ECD), we consider a modeling pipeline as illustrated in Figure 2b. For convenience, we refer to this model as DenseNetCD. Because the alternative model leverages the feature presentation method that prior works consider the best and is equipped with an identical classifier as the E2ECD model, we shall use it as a baseline model to compare with the E2ECD model.

## 4. Evaluation

### 4.1. Evaluation Data Sets

We prepare two data sets by extracting Quack test records from Censored Planet [20]. One data set is for training and evaluating the latent feature learning model while the other for training and evaluating censorship detection. For convenience, we refer to the former data set as Data Set FL while the later Data Set CD.

It is important to note that Censored Planet organizes their data based on tests it runs. Specifically, each test is defined by its test request sent from a vantage point, and this test is to run multiple times, which results in multiple responses for the same test request message. On Censored Planet, a record consists of the metadata about the test request message and the multiple response messages. We flatten each Censored Planet test record by iteratively pairing the top level request metadata with each response message to create a record, essentially a record akin to a single request-response pair. This is to match the intended use of the system, i.e., for each request sent, we want to determine whether the request is censored based on the response received. In the remainder of this article, a test record is like a request-response pair as described, rather than a test record on Censored Planet.

Data Set FL consists of 1,369,071 response records of the tests that Censored Planet ran while Data Set CD consists of 1,711,339 vectors created as described in Section 3.1 paired

with metadata. The metadata consists of the domain or string under test, the IP address and country of the vantage point, timestamp for the test, and a flag value for censored, uncensored or undetermined.

Censored Planet matches each test response with a censorship fingerprint written in regular expression [51] and assigns a label to each test record. The label can be either “censored”, “uncensored”, or “undetermined”. It is worth noting that the latent feature representation learning model in Section 3.2 is an unsupervised learning model, as such, the label is irrelevant and unused. However, the censorship classification model in Sections 3.3 and 3.4 are supervised models and the labels are necessary for training and also serve as the “ground truth” for evaluation.

Table 1 summarizes useful statistics for the two data sets.

Table 1: Evaluation Data Sets

Data Set FL (for Feature Learning)	
# of Training Records	1,197,937
# of Validation Records	171,134
Total	1,369,071
Data Set CD (for Censorship Detection)	
# of Censored Records	215,016
# of Uncensored Records	653,481
# of Undetermined Records	842,842
Total	1,711,339

#### 4.2. Baseline Model

We treat the alternative model in Section 3.4 as a baseline mode, and discuss its evaluation first here. We expand the vector in each record in Data Set CD to an vector of length  $224 \times 224$  by padding each end of the byte sequence with zeros if necessary, export the vector to bytes and treat each vector as a gray-scale image. The training and evaluating settings are similar to those for the CD Classifier discussed in Section 4.4.1 later. These include the hold-out evaluation setting, i.e., we randomly partition the data set into three partitions, 70% of the data for training, 10% for validation, and 20% for testing. In addition, we use a learning rate scheduler that varies the learning rate between  $1 \times 10^{-6}$  and  $1 \times 10^{-7}$ . The scheduler is a cosine annealing strategy [52] with period of 10 epochs. We monitor the training processing using the validation loss and accuracy as shown in Figure 5a and Figure 5b. The trained network resulted in a loss of 0.048 on the test data with an accuracy of 0.986 where the accuracy is defined  $(TP + TN)/(P + N)$ .

#### 4.3. Feature Representation Learning

The Censor2Seq model described in Section 3.2 is to learn latent feature representation. Table 2 summarizes the hyperparameters of the Censor2Seq model used in this evaluation.

To evaluate the latent feature representation learning model, we use Data Set FL that is divided into a training and a validation data set (Table 1). Following the procedure in Section 3.1, we convert each test record in the data set to a sequence of numerical values represented as a numerical vector. This process

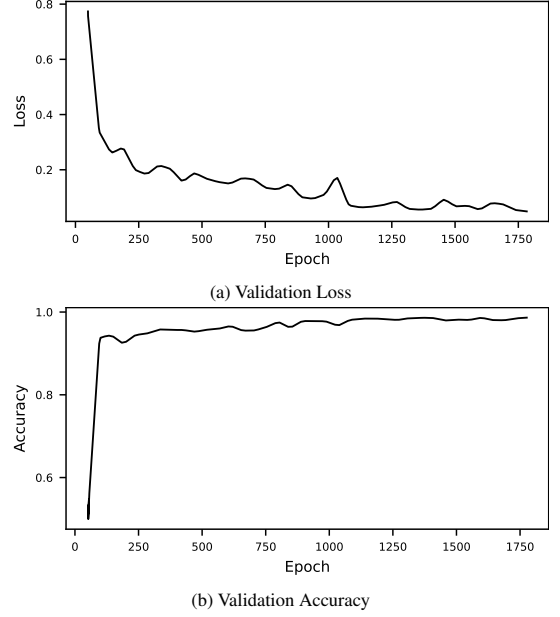


Figure 5: Validation loss and accuracy over training epochs

is described in Section 3.1 in which we detail how the largest token value in our vectors is 7,069. This value is used to define the embedding range.

For embedding size, we experiment with a number of values with a consideration on memory requirement, processing time, and convergence, find that the acceptable values range from 96 to 128, and settle at size 96.

Table 2: Hyperparameters of Censor2Seq Model

Hyperparameter	Value
size of input sequence size	7,069
embedding dimension	96
encoder hidden layer size	128
encoder output layer size	96
decoder input layer size	96
decoder hidden layer size	128
decoder output sequence size	7,069

As shown in Table 1, we partition the data set into two subsets, one for training and the other for validation. To reduce the demand of computational resources, such as, memory and CPU time, we adopt a statistical gradient descent (SGD) mini-batch training approach where we randomly sample 10% of training data, i.e., sample from 1,197,937 records at each training epoch and set batch size as 16. Following the best practice, we select a simple learning rate scheduler that uses a cosine annealing strategy [52] that decays learning rate smoothly from 0.003 to 0.0001 with period of 10 epochs.

We monitor the training process by checking on the entropy loss function value computed on the validation subset following each epoch. Following the selected early exit strategy, we stop the training process when the validation entry loss function value twice dipped below 20% of the initial entropy loss.



The validation loss function value over training epochs is in Figure 6.

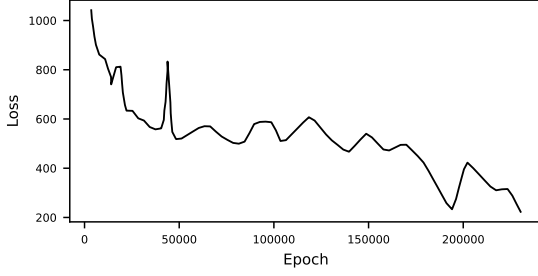


Figure 6: Validation loss of the Censor2Seq model.

The effectiveness of the Censor2Seq model is ultimately reflected by the quality of the lightweight numerical embeddings it produces. In the Section 4.4, we evaluate how effective the embeddings are to detect censorship events.

#### 4.4. Censorship Detection

Section 3.3 describes the classifier for censorship detection. It is a fully connected dense neural network. Table 3 is the hyperparameters of the neural network. This neural network is a supervised classification model that requires training.

Table 3: Hyperparameter of Censorship Detection Neural Network

Parameter	
input size	96
first layer size	512
second layer size	256
output layer size	2

##### 4.4.1. Training

We use Data Set CD to train the CD classifier. For each test record in Data Set CD, we process it using the trained Censor2Seq model. As a result, we obtain an embedding vector for each test record in Data Set CD. We adopt a hold-out evaluation strategy where we randomly partition the data set into three partitions, 70% of the data for training, 10% for validation, and 20% for testing.

As shown in Table 1, the censorship data here is unbalanced with regard to its label where there are 3 times as many responses identified as uncensored as those censored. We applied an approach of under-sampling the majority class to balance the training dataset whenever labeled data are needed, i.e., during the training we randomly under-sample the training data from the uncensored records, the majority class to match the censored records, the minority class.

The learning rate scheduler uses a cosine annealing strategy [52] with the period of 10 epochs and varies the learning rate between  $1 \times 10^{-6}$  and  $1 \times 10^{-7}$ . To prevent overfitting, we check the entropy loss value computed on the validation data after each training epoch and stop training when the validation loss ceases to reduce. We aid this by using an early stopping

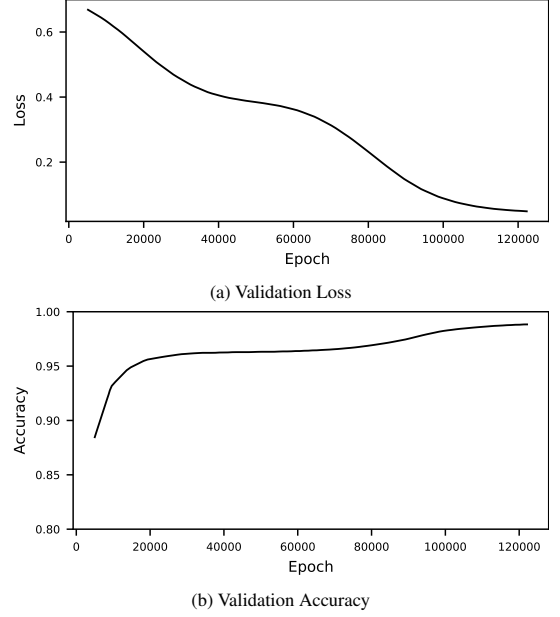


Figure 7: Validation loss and accuracy of the CD classifier over training epoch

strategy to eliminate unnecessary excessive training time. Figures 7a and 7b illustrate the validation loss and the classification accuracy over training epochs.

##### 4.4.2. Testing

Finally, to evaluate the effectiveness of the classifier, a surrogate to the effectiveness of the embeddings produced by the trained Censor2Seq model, we classify the test data set with the trained classifier. The classifier results in a loss of 0.047 and an accuracy of 0.988 where the accuracy is defined  $(TP + TN)/(P + N)$ .

Table 4: Comparison of Classification Accuracy of E2ECD and DenseNetCD

Model	Loss	Accuracy
E2ECD	0.047	0.988
DenseNetCD	0.048	0.986

Table 4 summarizes and compares the evaluation results of this model and the baseline model. The classification performance of the two models are close if not considered identical. However, the E2ECD model has a clear advantage when it comes to classifying undetermined test records as discussed in Section 4.5.

#### 4.5. Censorship Detection on Undetermined Records

Data Set CD contains a 842,842 test records labeled as undetermined as discussed in Section 4.1. We are interested to know whether there are censorship events in this set of undetermined test records. For this, we classify the records using both the trained CD Classifier and DenseNetCD models. There is a striking difference between the results of the models as shown in Table 5. To interpret the result, it is necessary to understand the measurement tests performed by Centered Planet.

*Background.* The data records in Data Set CD are from Quack tests [32]. Two major phases of a Quack test are “Retry” and “Control”. In the “Retry” phase, the platform has an Echo request with a potentially offending payload repeatedly sent by a vantage point, e.g., sent 5 times with a delay in between. When all requests result in a failure, the platform carries out the Control phase where the platform has an Echo request with an innocuous payload sent by the vantage point. Only when this Echo request fails, the test declares that there might be a network reachability problem due to network interference.

Quack is effectively detecting the network reachability resulted from network interference [32]. However, not all of the network interference detected by Quack is censorship. The exceptions include server-side blocking errors (e.g., HTTP Status Code 403), page-not-found errors (e.g., HTTP Status Code 404), and DDOS checks on some domains [44]. In addition, a recent investigation also indicates that some Censored Planet test requests were not sent successfully, which could also lead to unexpected responses [21].

Table 5: Comparison of Classification Results on Undetermined Tests

Model	Probable Censorship	Probable%
E2ECD	557,492	66.14%
DenseNetCD	183	0.02%

*Analysis of the Results.* Which model is more accurate? Our answer is not definite; however, it is more likely that the CD Classifier produces more meaningful results, in particular, when considering the design of Quack, we expect a significant proportion of the undetermined records should be the results of censorship. Aiming to confirm this, we divided each of the results into groups based on the patterns of the data records. Table 6 summarizes the grouping of the classification result of the E2ECD model while Table 7 that of the DenseNetCD model.

The E2ECD model via the CD Classifier yields far more censorship detections. We can confirm with a high confidence that some of these results are indeed probable censorship events. For instance, groups 1–3 and 5–7 in Table 6 are the block pages of Internet filters (or Firewalls), such as, Bitdefender, Cisco Meraki, and Seqrite Endpoint Security, and in total, the 1,184 responses that are likely actual censorship block pages by examining the patterns of the these block pages. Similarly, the 122 responses in group 4 that are an *HTTP Code 302* response are also likely the result of censorship

Most of the remaining records are likely the result of censorship. An investigation on the Great Firewall of China indicates that both *connection reset by peer* and *connection timed out* are among its observable characteristics [53]. As discussed in the above, the response to the request sent to these vantage points have been verified with innocuous payloads, and therefore it is very unlikely that the network has unexpectedly and repeatedly failed during these specific queries.

Table 7 summarizes the grouping of the result of the DenseNetCD model. There are far fewer results shown and all of them are block pages or *HTTP Code 302*. Clearly the ability

of the DenseNetCD model to discover new censorship events is questionable.

We hypothesize that the difference between the models lie at the distinction of the designs of the two approaches. DenseNet is designed for per-pixel prediction models. As indicated in a recent study [54], the state-of-the-art per-pixel classification model underperforms mask classification models in image semantic segmentation tasks where the mask classification models disentangle the image partitioning and classification aspects of image segmentation. There is a parallel when it comes to the two censorship detection models we proposed. The E2ECD model separates the censorship detection into two tasks, feature representation learning and censorship detection while the DenseNetCD model bundles the two together. Additionally, the encoding method used by Censorship2Seq is also designed to encode the relationships between the individual tokens while an image classifier is intended to be aware of clusters of pixels, it is less aware of connections between distant pixels. Due to the design of the feature representation learning model and the disentanglement of the two tasks, E2ECD fares better than DenseNetCD, as a result of more generalizable feature presentation learned by Censorship2Seq. It is also highly likely that the DenseNetCD model learned highly idiosyncratic features specific to the training data, resulting in poor generalizability, and notably the phenomenon of this nature has also been reported in studies using deep learning models in other areas, such as, vulnerability prediction [55].

## 5. Limitations and Threats to Validity

This work is on the design and the evaluation of an “end-to-end” network-based Internet censorship detection using deep learning. In particular, we advocate and argue that there is a strength in the approach that uses latent feature represent learning in embedding space. Deep learning is not clairvoyant and there can be threats to validity and limitations that constrain the potential of this work. Here, we discuss several of these limitations.

*Data.* We selected Censored Planet as the source of the evaluation data and extracted Quack test data from it. Because Quack [32, 44] monitors network side-channels, as we discussed in Section 2, the censorship events detected are unambiguously network-based Internet censorship.

There is a threat to internal validity stemmed from the quality of the evaluation data. A recent study indicates that a significant portion of the Quack tests did not successfully transmit a test request in the first place and resulted in false block pages [21].

However, this impacts our results little. Since these false block pages are not to be identified as a censorship and are invalid pages, there is no impact on the quality of the test records that are labeled as censorship and our trained models can recognize almost all the correctly identified censorship events as shown in Table 4.

*Hyperparameter and Model Tuning.* The predictive performance of the deep learning models like those investigated in

Table 6: Censorship Candidates from E2DCD

No.	Type	Frequency	Locations
1.	ATT block page	3	United States
2.	Bitdefender Alert Page block page	1,133	India, United States
3.	Extra Safe Internet block page	4	Netherlands
4.	HTTP code 302	122	Belarus, China, Kazakhstan, Pakistan, Russia
5.	Meraki block page	1	Singapore
6.	Seqrite Endpoint Security block page	37	India
7.	Net Protector block page	6	India
8.	'Connection: close' message returned without block page	10	China, U.S. Virgin Islands, United States
9.	'connection reset by peer' error	542,083	Bangladesh, Brunei, Canada, China, Colombia, Egypt, Ethiopia, Germany, Hong Kong, India, Iran, Ivory Coast, Kenya, Libya, Mexico, Oman, Pakistan, Poland, Qatar, Russia, Saudi Arabia, Singapore, South Korea, Syria, Taiwan, Turkey, United Arab Emirates, United States, Uzbekistan, Vietnam
10.	'no route to host' error	296	Argentina, Australia, Bangladesh, Belgium, Brazil, Colombia, Czechia, Germany, Greece, India, Indonesia, Italy, Japan, Libya, Malaysia, Mexico, Moldova, Nepal, Poland, South Korea, Spain, Switzerland, Taiwan, Thailand, United Kingdom, United States
11.	'connection timed out' error	2,885	Angola, Argentina, Austria, Bangladesh, Brazil, Burundi, Canada, China, Colombia, Czechia, Germany, Greece, Guadeloupe, India, Iran, Italy, Japan, Mexico, Netherlands, Nigeria, Philippines, Russia, South Africa, South Korea, Spain, Sweden, Switzerland, Taiwan, Turkey, U.S. Virgin Islands, Ukraine, United Kingdom, United States
12.	'I/O timeout' error	6,983	Algeria, Armenia, Bangladesh, Belarus, Belgium, Brazil, Burundi, Canada, China, Egypt, Germany, Guam, Hong Kong, India, Indonesia, Iran, Kazakhstan, Kenya, Madagascar, Malaysia, Mexico, Netherlands, Nigeria, Oman, Pakistan, Paraguay, Qatar, Romania, Russia, Saudi Arabia, South Korea, Taiwan, Tanzania, Thailand, Turkey, United Kingdom, United States, Uzbekistan, Vietnam, Zambia
13.	'network is unreachable' error	18	Indonesia, Poland
14.	'connection refused' error	3,007	Bangladesh, Brazil, Chile, China, Colombia, Czechia, Egypt, France, Germany, Greece, India, Italy, Ivory Coast, Japan, Kenya, Mexico, Nepal, Pakistan, Peru, Poland, Russia, Singapore, South Africa, South Korea, Spain, Sri Lanka, Sweden, Taiwan, Thailand, Ukraine, United States
15.	'echo response does not match echo request' and no other data	904	Algeria, Armenia, Bangladesh, Belarus, Belgium, Brazil, Burundi, Canada, China, Egypt, Germany, Guam, Hong Kong, India, Indonesia, Iran, Kazakhstan, Kenya, Madagascar, Malaysia, Mexico, Netherlands, Nigeria, Oman, Pakistan, Paraguay, Qatar, Romania, Russia, Saudi Arabia, South Korea, Taiwan, Tanzania, Thailand, Turkey, United Kingdom, United States, Uzbekistan, Vietnam, Zambia

Table 7: Censorship Candidates from DenseNetCD

No.	Type	Frequency	Locations
1.	ATT block page	3	United States
2.	Bitdefender Alert Page block page	116	India, United States
3.	Extra Safe Internet block page	1	Netherlands
4.	HTTP code 302	62	China, Kazakhstan, Pakistan, Russia
5.	Meraki block page	1	Singapore

this study is subject to the choice of hyperparameters [56]. Due to the computation resources available to us, we were unable to experiment exhaustively on a large collection of hyperparameters. However, we took measures to ensure the evaluation settings of the proposed E2ECD and the DenseNetCD models are comparable. First, we adopted an identical training strategy, i.e., the Stochastic Gradient Descent with the cosine annealing learning rate scheduler with similar configuration. Second, we use an identical hold-out evaluation setting. Finally, we identify a pre-trained DenseNet that represents the state-of-the-art to design the baseline model. The proposed E2ECD model yields an almost identical prediction accuracy as the baseline model on the test data set (Table 4). We are convinced that the latent feature presentation model presented here has an appropriate design.

Despite this, we recognize that we used the smallest of the DenseNet architectures, also known as DenseNet 121 due to the constraint of computational resources available to us. The original DenseNet research found that larger DenseNets had a lower error rate on the ImageNet classification problem [45], as such, larger DenseNets may also be more effective at detecting censorship.

*Censorship Detection on Undetermined Test Records.* To compare the E2ECD and the DenseNetCD models, we also test them on a set of undetermined test records. The E2ECD model detects far more candidate censorship events than the DenseNetCD model. We argue that it is likely the result of the advantage of the latent feature representation approach. The undetermined test records are all perceived network outages. First, it is clear that we are unable to access the intention of any factors that might cause these outages. Second, we are limited by our knowledge to determine whether the outages are truly censorship or ordinary network outages. As the result, the reliability of our assessment is not absolute.

Because the evaluation data set contains in total 842,842 records, a thorough examination of the prediction results manually is infeasible. We plan to study these test records in a future work. Because we are unable to access people’s intention who might initiate the censorship events, the correctness of censorship detection is often via cross-examination and inference. For this, we plan to compare records collected by multiple Internet censorship measurement platforms including both the Censored Planet and ICLab in the same time period [20, 21]. Second, following the approach adopted by prior works, we shall cluster the test records, such as, those predicted as probable censorship events, and manually examine each cluster to determine whether the prediction is correct by inferring what the censorship mechanism is and what intention of censorship may be [20, 21, 27].

*E2ECD versus DenseNetCD.* We argue that the E2ECD model is superior to the DenseNetCD model; however, the E2ECD model is not without a limitation when compared to the DenseNetCD model. The E2ECD model requires training two neural network models, a feature representation learning model and a classification model. In contrast, the DenseNetCD model

only needs to train a single pre-trained DenseNet. We observe that training the two networks of the E2ECD model requires inherently more computation than training a single network of DenseNetCD. The E2ECD model took far more iterations to train, more than 100 times the number of steps as our DenseNetCD model. In addition, the Censor2Seq component of the E2ECD model is far more complex and so requires more computation per training step. However, we argue that this additional complexity is clearly worth the computation cost given the striking difference between the abilities of the two models as discussed in Section 4.5.

*Replication Package.* Some unmitigated limitations and threats to validity discussed in the above necessitate a future exploration along those directions. Ultimately, the approach to examine these limitations and threats to validity is via replication studies. To facilitate this, we compose a replication package and make it publicly available [37]. This package can also be useful to serve as a research baseline, to extend our work, and to help develop fully automated censorship detection systems.

## 6. Conclusion and Discussion

We examine a design of a fully-automated network-based Internet censorship detection system. There are primarily three challenges we must address: to process an overwhelmingly large quantity of structured network measurement data for censorship detection, to extract high quality features from this data, and to address the challenge of the lack of training data for the proposed supervised learning approach. Our contributions are therefore as follows.

First, we engineer an iterative data processing Python library that allows us stream the network measurement data directly from its cloud storage. Second, recognizing the importance of the structure and the order of elements in the network measurement data, we design an unsupervised sequence-to-sequence deep learning model to infer latent feature represents in embedding space from the data. Third, we prepare a training dataset using known fingerprints of network-based Internet censorship. Fourth, due to the lack of machine learning approaches of network-based Internet censorship detection in the literature, we build two complete censorship detection models, one based on feature representation learning, and the other based on image classification, and compare the predictive performance of the two models. As a result, the work resulted in an “end-to-end” network-based Internet censorship detection pipeline accompanied by a replication package publicly available for adoption and extension.

*Discussion.* A worthy lesson is that there is a cyclic dependency or chicken-egg problem when it comes to the design of the “end-to-end” censorship detection system. Such a system shall be based on a supervised learning algorithm that requires a large set of training network measurement test records labeled as “censored” or “uncensored” to learn to detect censorship;

however, we need to be able to recognize what constitutes censorship by examining these data records. As a result, the cyclic dependency problem emerges.

In this work, we leverage a set of censorship fingerprints in the form of regular expressions and the censorship scanning scripts available by Censored Planet. The scripts use regular expressions to match received block page responses, which requires discovering and analyzing such responses, then designing a regular expression based on that analysis. This limits censorship detection to patterns already discovered. However, our work indicates that the labeled data set generated in this process is more than appropriate to serve as the required training dataset. Indeed, our research affirms that a machine learning model can learn to detect previously unseen block pages. Both of our two experimental models (E2ECD and DenseNetCD) detected block page responses that do not match any of the regular expressions provided in the scanning scripts from Censored Planet. Further, our E2ECD model with sequence-to-sequence latent feature representation learning identified as probable censorship several types of responses that do not correlate to simple textual patterns and therefore would be very difficult if not impossible to detect using regular expression based scripts. Additionally, There is a striking difference between the number of responses that the two deep learning methods (E2ECD and DenseNetCD) identify as probable censorship. We conclude that a sequence-to-sequence autoencoder enhanced with an attention mechanism as proposed is far more effective at discovering censorship than the simple image feature representation method used by DenseNetCD.

An added benefit of our research is that our results show that useful latent feature representation of censorship measurement in embedding space can be identified by deep neural networks. We expect that the embeddings should be sufficient to identify new and known network-based censorship events. This is evident, as shown in our evaluation, the two experimental networks displayed an accuracy better than 98% when processing responses that are already categorized by the scanning scripts. More significantly, both of our networks discovered censorship missed by these scripts, showing that deep neural networks can detect features not readily apparent. Although machine learning is no panacea, we are convinced that these deep learning networks have the potential to be a powerful tool to understand the constantly changing landscape of Internet censorship.

In addition, we only evaluate our model using the Censored Planet data set. As discussed in Section 2, there are now several complementary prominent large scale network measurement platforms for Internet censorship. Our future work includes the extension of the current model to handle and correlate both ordinary network traffic measurement and network side-channel measurement data from these complementary platforms. Additionally, there is significant and continuous development in modeling techniques. We expect that our models can be improved using these developments.

## Acknowledgement

This research was supported, in part, by a grant of computer time from the City University of New York High Performance Computing Center. This research was also supported, in part, by a grant of software as a service from Comet ML (<https://comet.ml>).

## References

- [1] G. Aceto, A. Pescapé, Internet censorship detection: A survey, *Computer Networks* 83 (2015) 381–421. doi:10.1016/j.comnet.2015.03.008.  
URL <https://www.sciencedirect.com/science/article/pii/S1389128615000948>
- [2] T. Zhu, D. Phipps, A. Pridgen, J. R. Crandall, D. S. Wallach, The velocity of censorship: {High-Fidelity} detection of microblog post deletions, in: 22nd USENIX Security Symposium (USENIX Security 13), 2013, pp. 227–240.
- [3] D. Xue, R. Ramesh, A. Jain, M. Kallitsis, J. A. Halderman, J. R. Crandall, R. Ensafi, OpenVPN is open to VPN fingerprinting, in: 31st USENIX Security Symposium (USENIX Security 22), USENIX Association, Boston, MA, 2022, pp. 483–500.  
URL <https://www.usenix.org/conference/usenixsecurity22/presentation/xue-diwen>
- [4] A. Dainotti, C. Squarcella, E. Aben, K. C. Claffy, M. Chiesa, M. Russo, A. Pescapé, Analysis of country-wide Internet outages caused by censorship, in: Proceedings of the 2011 ACM SIGCOMM conference on Internet measurement conference, 2011, pp. 1–18.
- [5] G. Aceto, A. Botta, P. Marchetta, V. Persico, A. Pescapé, A comprehensive survey on Internet outages, *Journal of Network and Computer Applications* 113 (2018) 36–63.
- [6] P. Winter, S. Lindskog, How the Great Firewall of China is blocking Tor, in: 2nd USENIX Workshop on Free and Open Communications on the Internet, Bellevue, WA, USENIX-The Advanced Computing Systems Association, 2012, p. 7.
- [7] Z. Chai, A. Ghafari, A. Houmansadr, On the importance of Encrypted-SNI (ESNI) to censorship circumvention, in: 9th USENIX Workshop on Free and Open Communications on the Internet (FOCI 19), 2019.
- [8] S. Satija, R. Chatterjee, BlindtLS: Circumventing TLS-based https censorship, in: Proceedings of the ACM SIGCOMM 2021 Workshop on Free and Open Communications on the Internet, 2021, pp. 43–49.
- [9] A. Shishkina, L. Issaev, Internet censorship in Arab countries: Religious and moral aspects, *Religions* 9 (11) (2018) 358.
- [10] S. A. Meserve, D. Pemstein, Google politics: The political determinants of Internet censorship in democracies, *Political Science Research and Methods* 6 (2) (2018) 245–263.
- [11] P. Chen, Pornography, protection, prevarication: the politics of Internet censorship., *University of New South Wales Law Journal* 23 (1) (2000) 221–226.
- [12] S. Aryan, H. Aryan, J. A. Halderman, Internet censorship in Iran: A first look, in: 3rd USENIX Workshop on Free and Open Communications on the Internet (FOCI 13), 2013.
- [13] Z. Nabi, The anatomy of Web censorship in Pakistan, in: 3rd USENIX Workshop on Free and Open Communications on the Internet (FOCI 13), 2013.
- [14] R. Singh, R. Nithyanand, S. Afroz, P. Pearce, M. C. Tschantz, P. Gill, V. Paxson, Characterizing the nature and dynamics of Tor exit blocking, in: 26th USENIX Security Symposium (USENIX Security 17), 2017, pp. 325–341.
- [15] T. K. Yadav, A. Sinha, D. Gosain, P. K. Sharma, S. Chakravarty, Where the light gets in: Analyzing Web censorship mechanisms in India, in: Proceedings of the Internet Measurement Conference 2018, 2018, pp. 252–264.
- [16] K. Y. Ng, A. Feldman, C. Leberknight, Detecting censorable content on Sina Weibo: A pilot study, in: Proceedings of the 10th Hellenic Conference on Artificial Intelligence, 2018, pp. 1–5.
- [17] K. Bock, G. Naval, K. Reese, D. Levin, Even censors have a backup: Examining China’s double HTTPS censorship middleboxes, in: Proceedings

- of the ACM SIGCOMM 2021 Workshop on Free and Open Communications on the Internet, 2021, pp. 1–7.
- [18] R. Padmanabhan, A. Filastò, M. Xynou, R. S. Raman, K. Middleton, M. Zhang, D. Madory, M. Roberts, A. Dainotti, A multi-perspective view of Internet censorship in Myanmar, in: Proceedings of the ACM SIGCOMM 2021 Workshop on Free and Open Communications on the Internet, 2021, pp. 27–36.
  - [19] V. Ververis, T. Ermakova, M. Isaakidis, S. Basso, B. Fabian, S. Milan, Understanding Internet censorship in Europe: The case of Spain, in: 13th ACM Web Science Conference 2021, 2021, pp. 319–328.
  - [20] R. Sundara Raman, P. Shenoy, K. Kohls, R. Ensafi, Censored Planet: An Internet-wide, Longitudinal Censorship Observatory, in: Proceedings of the 2020 ACM SIGSAC Conference on Computer and Communications Security, CCS '20, Association for Computing Machinery, New York, NY, USA, 2020, pp. 49–66. doi:10.1145/3372297.3417883. URL <http://doi.org/10.1145/3372297.3417883>
  - [21] A. A. Niaki, S. Cho, Z. Weinberg, N. P. Hoang, A. Razaghpanah, N. Christin, P. Gill, ICLab: A global, longitudinal Internet censorship measurement platform, in: 2020 IEEE Symposium on Security and Privacy (SP), IEEE, 2020, pp. 135–151.
  - [22] A. Filastò, J. Appelbaum, OONI: Open observatory of network interference, in: 2nd USENIX Workshop on Free and Open Communications on the Internet (FOCI 2012), 2012.
  - [23] L. Qiao, X. Li, Q. Umer, P. Guo, Deep learning based software defect prediction, *Neurocomputing* 385 (2020) 100–110.
  - [24] G. Lin, S. Wen, Q.-L. Han, J. Zhang, Y. Xiang, Software vulnerability detection using deep neural networks: a survey, *Proceedings of the IEEE* 108 (10) (2020) 1825–1848.
  - [25] X. Gao, M. Qiu, M. Liu, Machine learning based network censorship, in: 2021 8th IEEE International Conference on Cyber Security and Cloud Computing (CSCloud)/2021 7th IEEE International Conference on Edge Computing and Scalable Cloud (EdgeCom), IEEE, 2021, pp. 149–154.
  - [26] J. Li, Predicting large-scale Internet censorship—a machine learning approach, Master's thesis, the School of Engineering and Applied Science, the University of Virginia, available: <https://libra2.lib.virginia.edu/downloads/d504rk52c> (2015).
  - [27] B. Jones, T.-W. Lee, N. Feamster, P. Gill, Automated detection and fingerprinting of censorship block pages, in: Proceedings of the 2014 Conference on Internet Measurement Conference, 2014, pp. 299–304.
  - [28] R. S. Raman, A. Stoll, J. Dalek, R. Ramesh, W. Scott, R. Ensafi, Measuring the deployment of network censorship filters at global scale., in: NDSS, 2020.
  - [29] P. Pearce, R. Ensafi, F. Li, N. Feamster, V. Paxson, Augur: Internet-wide detection of connectivity disruptions, in: 2017 IEEE Symposium on Security and Privacy (SP), IEEE, 2017, pp. 427–443.
  - [30] P. Pearce, B. Jones, F. Li, R. Ensafi, N. Feamster, N. Weaver, V. Paxson, Global measurement of DNS manipulation, in: 26th USENIX Security Symposium (USENIX Security 17), 2017, pp. 307–323.
  - [31] W. Scott, T. Anderson, T. Kohno, A. Krishnamurthy, Satellite: Joint analysis of CDNs and Network-Level interference, in: 2016 USENIX Annual Technical Conference (USENIX ATC 16), 2016, pp. 195–208.
  - [32] B. VanderSloot, A. McDonald, W. Scott, J. A. Halderman, R. Ensafi, Quack: Scalable remote measurement of Application-Layer censorship, in: 27th USENIX Security Symposium (USENIX Security 18), 2018, pp. 187–202.
  - [33] L. Jin, S. Hao, H. Wang, C. Cotton, Understanding the practices of global censorship through accurate, end-to-end measurements, *Proceedings of the ACM on Measurement and Analysis of Computing Systems* 5 (3) (2021) 1–25.
  - [34] U. Trivedi, M. Patel, A fully automated deep packet inspection verification system with machine learning, in: 2016 IEEE International Conference on Advanced Networks and Telecommunications Systems (ANTS), IEEE, 2016, pp. 1–6.
  - [35] A. Sarabi, M. Liu, Characterizing the Internet Host Population Using Deep Learning: A Universal and Lightweight Numerical Embedding, in: Proceedings of the Internet Measurement Conference 2018, IMC '18, Association for Computing Machinery, New York, NY, USA, 2018, pp. 133–146. doi:10.1145/3278532.3278545. URL <http://doi.org/10.1145/3278532.3278545>
  - [36] A. Aizman, G. Maltby, T. Breuel, High Performance I/O For Large Scale Deep Learning, in: 2019 IEEE International Conference on Big Data (Big Data), Institute of Electrical and Electronics Engineers, Los Angeles, CA, 2019, pp. 5965–5967. doi:10.1109/BigData47090.2019.9005703.
  - [37] Shawn P. Duncan, Replication package for network-based internet censorship detection (May 2022). URL [https://github.com/FatherShawn/cp\\_learning](https://github.com/FatherShawn/cp_learning)
  - [38] A. Conneau, K. Khandelwal, N. Goyal, V. Chaudhary, G. Wenzek, F. Guzmán, É. Grave, M. Ott, L. Zettlemoyer, V. Stoyanov, Unsupervised cross-lingual representation learning at scale, in: Proceedings of the 58th Annual Meeting of the Association for Computational Linguistics, 2020, pp. 8440–8451.
  - [39] D. J. Rezende, S. Mohamed, D. Wierstra, Stochastic backpropagation and approximate inference in deep generative models, in: International conference on machine learning, PMLR, 2014, pp. 1278–1286.
  - [40] M.-T. Luong, H. Pham, C. D. Manning, Effective approaches to attention-based neural machine translation, in: Proceedings of the 2015 Conference on Empirical Methods in Natural Language Processing, 2015, pp. 1412–1421.
  - [41] E. Raff, Inside Deep Learning: Math, Algorithms, Models, Manning Publications Co., Shelter Island, New York, 2021.
  - [42] T. Mihaylova, A. F. T. Martins, Scheduled sampling for transformers, in: Proceedings of the 57th Annual Meeting of the Association for Computational Linguistics: Student Research Workshop, Association for Computational Linguistics, Florence, Italy, 2019, pp. 351–356. doi:10.18653/v1/P19-2049. URL <https://aclanthology.org/P19-2049>
  - [43] Z. Niu, G. Zhong, H. Yu, A review on the attention mechanism of deep learning, *Neurocomputing* 452 (2021) 48–62.
  - [44] R. S. Raman, A. Stoll, J. Dalek, R. Ramesh, W. Scott, R. Ensafi, Measuring the Deployment of Network Censorship Filters at Global Scale, in: Proceedings 2020 Network and Distributed System Security Symposium, Internet Society, San Diego, CA, 2020, pp. 1–16. doi:10.14722/ndss.2020.23099. URL <https://www.ndss-symposium.org/wp-content/uploads/2020/02/23099.pdf>
  - [45] G. Huang, Z. Liu, L. Van Der Maaten, K. Q. Weinberger, Densely Connected Convolutional Networks, in: 2017 IEEE Conference on Computer Vision and Pattern Recognition (CVPR), Curran Associates Inc., Honolulu, Hawaii, USA, 2017, pp. 2261–2269. doi:10.1109/CVPR.2017.243.
  - [46] Li Fei-Fei, ImageNet Large Scale Visual Recognition Challenge 2012 (ILSVRC2012) (May 2012). URL <https://image-net.org/challenges/LSVRC/2012/>
  - [47] J. Hemalatha, S. A. Roseline, S. Geetha, S. Kadry, R. Damaševičius, An Efficient DenseNet-Based Deep Learning Model for Malware Detection, *Entropy* 23 (3) (2021) 344. doi:10.3390/e23030344. URL <https://www.mdpi.com/1099-4300/23/3/344>
  - [48] J. Chen, K. Hu, Y. Yu, Z. Chen, Q. Xuan, Y. Liu, V. Filkov, Software visualization and deep transfer learning for effective software defect prediction, in: Proceedings of the ACM/IEEE 42nd international conference on software engineering, 2020, pp. 578–589.
  - [49] Y. Zhu, S. Newsam, Densenet for dense flow, in: 2017 IEEE international conference on image processing (ICIP), IEEE, 2017, pp. 790–794.
  - [50] Pytorch Team, DenseNet, available: [https://pytorch.org/hub/pytorch\\_vision\\_densenet/](https://pytorch.org/hub/pytorch_vision_densenet/), retrieved August 31, 2021.
  - [51] Sarah Laplante, Blockpage and False Positive Signatures from Censored Planet Analysis (Apr. 2021). URL <https://github.com/censoredplanet/censoredplanet-analysis/tree/master/pipeline/metadata/data>
  - [52] I. Loshchilov, F. Hutter, SGDR: Stochastic gradient descent with warm restarts, in: Proceedings of the 5th International Conference on Learning Representations, 2017. URL <https://openreview.net/forum?id=Skq89Scxx>
  - [53] A. Shu, Data Mining of Chinese Social Media, Thesis, Rice University, accepted: 2016-01-25T21:29:03Z (Oct. 2014). URL <https://scholarship.rice.edu/handle/1911/88119>
  - [54] B. Cheng, A. Schwing, A. Kirillov, Per-pixel classification is not all you need for semantic segmentation, *Advances in Neural Information Processing Systems* 34 (2021) 17864–17875.
  - [55] S. Chakraborty, R. Krishna, Y. Ding, B. Ray, Deep learning based vulnerability detection: Are we there yet, *IEEE Transactions on Software Engineering* (2021).

- [56] L. Yang, A. Shami, On hyperparameter optimization of machine learning algorithms: Theory and practice, *Neurocomputing* 415 (2020) 295–316.